Crystal and Molecular Structures of Silyl Isocyanate (at —135 °C) and of Germyl Isocyanate (at —95 °C)

By **Michael J. Barrow, E. A. V. Ebsworth,** and **Marjorie M. Harding,** Department of Chemistry, Edinburgh University, West Mains Road, Edinburgh EH9 3JJ

Crystals of the title compounds are orthorhombic, space group *Pnma*, with $Z = 4$. For silyl isocyanate, $a = 7.96$, $b = 6.52$, and $c = 7.10$ Å (at −135 °C), while for germyl isocyanate $a = 8.01$, $b = 6.67$, and $c = 6.97$ Å (at −95 °C); 0.3% estimated standard deviations are assumed. Crystals have been grown '*in situ*' on a Weissenberg goniometer fitted with low-temperature equipment, and microdensitometer intensities obtained from films exposed using Cu-K_α radiation. The structures have been refined to $R = 0.034$ over 329 reflections for silyl isocyanate, and $R = 0.049$ over 266 reflections for germyl isocyanate. The compounds have similar crystal structures, involving crystallographic $C_s(m)$ molecular symmetry and bent (zigzag) heavy-atom skeletons. Important molecular parameters are: for silyl isocyanate, Si–N 1.720(6) Å, Si–N–C 158.4(5), and N–C–O 176.4(6)°; for germyl isocyanate, Ge–N 1.856(8) Å, Ge–N–C 147.0(7) and N–C–O 173.8(9)°. Both structures contain M · · · N and M · · · O intermolecular interactions. The nitrogen interactions result in linear N · · · M–N groupings and may be responsible for an apparent increase in the M–N bond length as compared with molecules in the gas phase. A quantitative method for estimating the increases to M–N bond lengths is described in the Appendix.

When trisilylamine was first prepared [1] its weakly basic character suggested unexpected differences between it and trimethylamine and subsequently an electron-diffraction (e.d.) study [2] showed that in trisilylamine the co-ordination around N is trigonal planar. The methyl pseudo-halides MeNCO and MeNCS have bent heavy-atom skeletons with angles at N (as measured by e.d.) of *ca.* 141°.[3] The first silyl derivative containing the NCY group (Y = O, S, or Se) to be characterised was $SiH_3(NCS)$:[4] the i.r. spectrum contained much resolved rotational detail, implying that the heavy-atom skeleton was linear. This implication was substantially confirmed by a detailed study of the microwave spectrum,[5] the apparent angle at N of 164° as determined by e.d. being ascribed to shrinkage associated with a skeletal bending mode of large amplitude.[6] The i.r. spectrum of gaseous $SiH_3(NCO)$ contains similar rotational detail, although the progressions are less well marked. Electron diffraction indicates an apparent angle at N of *ca.* 152°. From the shape of the Si · · · O peak in the radial distribution function it was deduced that the potential-energy (p.e.) function for the Si–N–C angle bending mode had a low hump at the linear configuration, the height of which approximated the energy of the lowest vibrational level.[6] The $SiH_3(NCO)$ molecule thus shows what has been described as 'pseudo-linear' or 'quasi-linear' behaviour. Subsequent detailed studies of the vapour-phase microwave spectrum [7] and of the low-frequency region of the i.r. spectrum [8] have confirmed the nature of the p.e. function and provided further information about the form of the potential. The compound $SiH_3(NCSe)$ has been less extensively studied; the Si–N–C angle is 158.9° by electron diffraction.[9]

Thus the compounds $SiH_3(NCY)$ have heavy-atom skeletons that are more or less linear but where the angle at N is easily deformed. The situation for the analogous germyl compounds is slightly different. Spectroscopic data for $GeH_3(NCS)$ can be interpreted in terms of a symmetric top with a Ge–N–C angle bend of large amplitude,[10] like $SiH_3(NCS)$, but the electron-diffraction [11] and spectroscopic data [12] for $GeH_3(NCO)$ appear consistent with a permanently bent structure with Ge–N–C 141° and there may be a more substantial barrier to adoption of linear geometry.

Most of the available evidence about the solid-state structures of these compounds has been inferred from vibrational spectroscopy. Fuller understanding of structural behaviour requires information about molecular geometries in the crystalline state to compare with the gas-phase geometries. With a low barrier to skeletal deformation, crystal forces may affect the intramolecular geometries; there is also the possibility of perturbations due to specific intermolecular interactions. Details of these distortions and 'secondary-bonding' effects provide additional insight into structural character. We have already found that in the crystal the pseudo-linear molecule disiloxane is bent with Si–O–Si 142.2(3)°, and that while solid disiloxane has weak but well defined O · · · Si intermolecular interactions, these interactions are not present in solid hexamethyldisiloxane where permethylation has presumably reduced the acceptor character of Si.[13]

We have attempted single-crystal preparations of $SiH_3(NCO)$, $SiH_3(NCS)$, $SiH_3(NCSe)$, $GeH_3(NCO)$, and $GeH_3(NCS)$. All these compounds are liquids at room temperature, are extremely sensitive to air and moisture, and most seem to suffer X-radiation damage. The growing and preservation of crystals for X-ray investigation has not proved easy. We here present the crystal structures of $SiH_3(NCO)$ and $GeH_3(NCO)$, the only two compounds where we have obtained single-crystal diffraction data. A preliminary account of the structure of $SiH_3(NCO)$ has already appeared.[14]

EXPERIMENTAL

Crystal Data.—(*a*) *Silyl isocyanate.* $SiH_3(NCO)$, $M = 73.1$, Orthorhombic, $a = 7.96$, $b = 6.52$, $c = 7.10$ Å [0.3% estimated standard deviations (e.s.d.s) assumed], $U = 368.5$ Å^3, $Z = 4$, $D_c = 1.32$ g cm^{-3}, Cu-K_α radiation (Ni-filter), $\lambda = 1.541\,8$ Å, μ(Cu-K_α) = 39.0 cm^{-1}, space group

Pnma (D_{2h}^{16}, no. 62) or *Pn2$_1$a* (C_{2v}^{9}, no. 33) by systematic absences, structure refined using the symmetry constraints of space group *Pnma*, m.p. −90 °C.

Cell parameters and intensities were measured at −135 °C. The final least-squares weighting scheme was $w^{-1} = 1 + 0.020(F_o - 7)^2$, and the final value of the isotropic extinction parameter $G = 3.8(3) \times 10^{-4}$, where $|F_c'| = |F_c|[1 + G|F_c|^2(1 + \cos^4 2\theta)/(1 + \cos^2 2\theta)\sin 2\theta]^{-\frac{1}{4}}$. The R factor was 0.034 over 329 reflections. A final difference-Fourier synthesis showed no peaks or troughs outside the range ±0.25 e Å^{-3}.

(*b*) *Germyl isocyanate.* $GeH_3(NCO)$, $M = 117.6$, Orthorhombic, $a = 8.01$, $b = 6.67$, $c = 6.97$ Å (0.3% e.s.d.s assumed), $U = 372.4$ Å^3, $Z = 4$, $D_c = 2.10$, Cu-K_α radiation with nickel-filter for incident beam and zinc filter for diffracted beam, $\lambda = 1.541\,8$ Å, μ(Cu-K_α) = 93.8 cm^{-1}, space group *Pnma* (D_{2h}^{16}, no. 62) or *Pn2$_1$a* (C_{2v}^{9}, no. 33) by systematic absences, structure refined using the symmetry constraints of space group *Pnma*, m.p. −45 °C.

Cell parameters and intensities were measured at −95 °C. The final least-squares weighting scheme was as in (*a*), but the final value of isotropic extinction parameter G was $2.6(2) \times 10^{-4}$. The R factor was 0.049 over 266 reflections. A final difference-Fourier synthesis showed peaks and troughs of ±1.2 e Å^{-3} close to germanium atoms and some other peaks and troughs of ±0.6 e Å^{-3} in regions between molecules.

Procedure.—Pure samples were sealed in Lindemann glass capillaries (internal diameter 0.5 mm) mounted on goniometer heads using heat-insulating Tufnol inserts. Single crystals suitable for X-ray investigation were grown '*in situ*' on a Nonius Weissenberg goniometer. The goniometer was fitted with Nonius low-temperature nitrogen-gas-stream equipment with some locally devised modifications. Intensity films were exposed for the Weissenberg levels *h*0—6*l* using Cu-K_α radiation and the multiple-film-pack method. During the collection of intensity data for the germyl compound a thin sheet of Zn metal was used as a 'diffracted-beam' filter (in addition to the incident-beam nickel-filter) to reduce the effects of Ge-K_α X-ray fluorescence.

Integrated intensities were derived from microdensitometer measurements performed by the S.R.C. Microdensitometer Service at Daresbury Laboratory, Warrington. The data were corrected for absorption effects using the SHELX program:[15] for each crystal a sufficient number of faces were defined in order to approximate the required shape (cylindrical) and orientation of the crystal. The intensities were further corrected for Lorentz and polarisation effects. For silyl isocyanate, 610 intensities were obtained from measurements of *hkl*, *hkl*, and *hkl* octants; after data reduction and merging of equivalent reflections, 330 unique reflections remained. Reflection 162 was consistently calculated with $F_c \gg F_o$ and was subsequently removed from the data so that the structure analysis utilized 329 reflections. Similarly for germyl isocyanate 505 intensities were measured which after merging yielded 278 unique reflections. The crystal of germyl isocyanate was of impaired quality: some reflection spots were split and the splitting was worse on the uppermost Weissenberg levels. In the event the *h*6*l* data were excluded from the structure refinement because of much reduced precision relative to the other data levels. The structure analysis was based on the 266 unique reflections from the levels *h*0—5*l*.

Structure Solution and Refinement.—For $Z = 4$ the space group *Pn2$_1$a* imposes no restriction on molecular symmetry, but *Pnma* would require the molecules to lie across the mirror planes at $y = \pm\frac{1}{4}$. Estimates of x/a and y/c co-ordinates for the Si (or Ge) atoms were obtained from Patterson syntheses. In both structures the heavy atom has an x/a co-ordinate of *ca.* $\frac{1}{4}$, so that the unit cell derived from the heavy-atom positions is pseudo-A-centred with the heavy atoms lying on positions of *mm* (C_{2v}) symmetry. The approximate orientations of the isocyanate groups could be inferred from weak features in the heavy-atom-phased F_o Fourier syntheses (using only reflections with $h + l$ even); this information, together with assumptions about bond lengths, was used to position the N, C, and O atoms. Both structures were then refined by least-squares calculations to minimise the quantity $\Sigma w(|F_o| - |F_c|)^2$ assuming the symmetry constraints of space group *Pnma*. There was never any indication from Fourier syntheses or from the atomic vibrations that the true space group was not centrosymmetric, but the possibility of slight distortions from $C_s(m)$ molecular symmetry cannot be excluded. Interlayer scale factors were assigned initially on the basis of exposure times. Only a single overall scale factor was varied during structure refinement. Improved individual layer scale factors were periodically evaluated by a least-squares method involving scaling the data level by level to the structure model. The positional and isotropic vibration parameters for hydrogen atoms were included in the refinement process, all hydrogen atoms having been unambiguously located from difference-Fourier syntheses. Anisotropic vibration parameters were included for all non-hydrogen atoms. During the refinement of germyl isocyanate the U parameter for H(1) persistently shifted to negative values and eventually this atom was refined with a fixed isotropic U of 0.03 Å^2. Empirical least-squares weighting schemes were introduced during the later stages of refinement. Empirical isotropic extinction corrections were applied by means of a variable parameter in the least-squares calculations (see *Crystal Data* above).

Atomic scattering factors for H atoms were from ref. 16, for Si (valence) and Ge from ref. 17(*a*), and for other elements from ref. 18. Allowance was made for the real and imaginary parts of the anomalous-dispersion effect for Ge and Si atoms.[17b] Calculations were performed using computers of the Edinburgh Regional Computing Centre and programs written here and the systems 'X-Ray '72',[19] SHELX,[15] and PLUTO.[20]

RESULTS

Final values of atomic parameters for silyl isocyanate and germyl isocyanate are given in Tables 1 and 2 respectively.

TABLE 1

Atomic parameters for $SiH_3(NCO)$ with estimated standard deviations in parentheses

Atom	x/a	y/b	z/c
Si	0.270 38(11)	0.25	0.167 74(12)
N	0.090 2(3)	0.25	0.034 0(5)
C	0.005 3(4)	0.25	−0.102 6(4)
O	−0.086 1(4)	0.25	−0.231 3(4)
H(1)	0.207(5)	0.25	0.342(6)
H(2)	0.349(3)	0.092(5)	0.132(4)

Details of the intramolecular and intermolecular geometries are given in Tables 3 and 4. Figure 1 shows a projection of the structure of silyl isocyanate down the *a* axis, Figure 2 the arrangement of molecules on the mirror plane at $y = \frac{1}{4}$.

TABLE 2

Atomic parameters for $GeH_3(NCO)$ with estimated standard deviations in parentheses

Atom	x/a	y/b	z/c
Ge	0.256 79(8)	0.25	0.191 22(10)
N	0.062 8(7)	0.25	0.045 6(8)
C	0.004 3(8)	0.25	−0.106 8(10)
O	−0.069 7(9)	0.25	−0.254 0(7)
H(1)	0.198(12)	0.25	0.362(11)
H(2)	0.357(7)	0.092(11)	0.152(9)

TABLE 3

Intramolecular geometry (with estimated standard deviations in parentheses)

		$SiH_3(NCO)$	$GeH_3(NCO)$
(a)	Distances (Å)		
	M–N	1.720(3)	1.856(6)
	N–C	1.183(4)	1.161(9)
	C–O	1.168(4)	1.185(9)
	M–H(1)	1.34(4)	1.28(8)
	M–H(2)	1.23(3)	1.35(7)
(b)	Angles (°)		
	M–N–C	158.4(3)	147.0(6)
	N–C–O	176.4(4)	173.8(8)
	N–M–H(1)	101.3(17)	101(4)
	N–M–H(2)	108.0(13)	113(3)
	H(1)–M–H(2)	112.6(16)	114(3)
	H(2)–M–H(2′)	113.4(19)	102(4)

The crystal structure of germyl isocyanate is similar and Figure 3 shows a superimposition of the two structures for molecules on the mirror planes at $y = \frac{1}{4}$. Tables of observed and calculated structure factors and thermal

TABLE 4

Intermolecular geometry (with estimated standard deviations in parentheses)

		$SiH_3(NCO)$	$GeH_3(NCO)$
(a)	Important intermolecular contacts (Å)		
	M · · · N^{I}	3.311(3)	3.062(6)
	M · · · O^{II}	3.303(3)	3.350(6)
(b)	Important intermolecular angles (°)		
	N–M · · · N^{I}	173.8(2)	176.3(2)
	H(1)–M · · · N^{I}	72(2)	75(4)
	H(2)–M · · · N^{I}	75(1)	69(3)
	M^{I}–N^{I} · · · M	106.7(1)	110.2(2)
	C^{I}–N^{I} · · · M	94.9(2)	103.0(5)
	N–M · · · O^{II}	76.7(1)	81.4(2)
	H(1)–M · · · O^{II}	178(2)	177(4)
	H(2)–M · · · O^{II}	68(1)	65(3)
	C^{II}–O^{II} · · · M	161.7(2)	174.5(6)
	N^{I} · · · M · · · O^{II}	109.5(1)	102.3(2)
(c)	Closest intermolecular contacts (Å) between light atoms		
	Shortest H · · · H		
	H(1) · · · $H(2^{III})$	3.04(5)	2.92(11)
	H(1) · · · $H(2^{IV})$	3.07(4)	3.08(9)
	Shortest H · · · C (or N or O)		
	C · · · $H(1^{III})$	3.01(4)	2.99(9)
	O · · · $H(2^{V})$	3.07(3)	3.03(6)
	O · · · $H(2^{VI})$	3.08(3)	2.92(7)
	N · · · $H(2^{III})$	3.22(3)	2.87(6)
	Shortest contacts between C, N, and O atoms		
	O · · · N^{V}	3.356(4)	3.578(9)
	C · · · N^{VII}	3.383(4)	3.405(10)
	O · · · C^{V}	3.460(4)	3.548(10)
	N · · · N^{VII}	3.595(6)	3.541(12)

Roman numerals as superscripts refer to the following equivalent positions relative to the reference molecule at x, y, z: I $\frac{1}{2}+x, y, \frac{1}{2}-z$; II $\frac{1}{2}+x, y, -\frac{1}{2}-z$; III $x-\frac{1}{2}, y, \frac{1}{2}-z$; IV $\frac{1}{2}-x, \frac{1}{2}+y, \frac{1}{2}+z$; V $x-\frac{1}{2}, y, -\frac{1}{2}-z$; VI $\frac{1}{2}-x, \frac{1}{2}+y, z-\frac{1}{2}$; VII $-x, -y, -z$

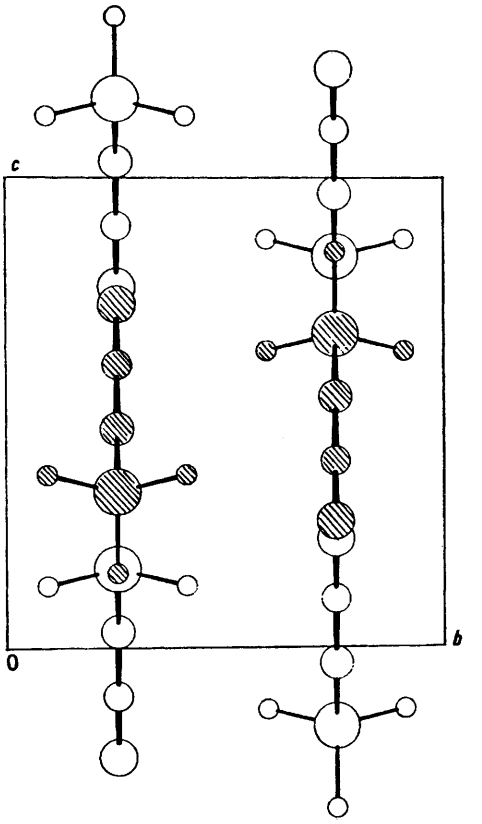

FIGURE 1 Crystal structure of $SiH_3(NCO)$ viewed down the a axis

parameters are available as Supplementary Publication No. SUP 22812 (7 pp.).*

The cell parameters are subject to the usual errors associated with the Weissenberg film method. These errors

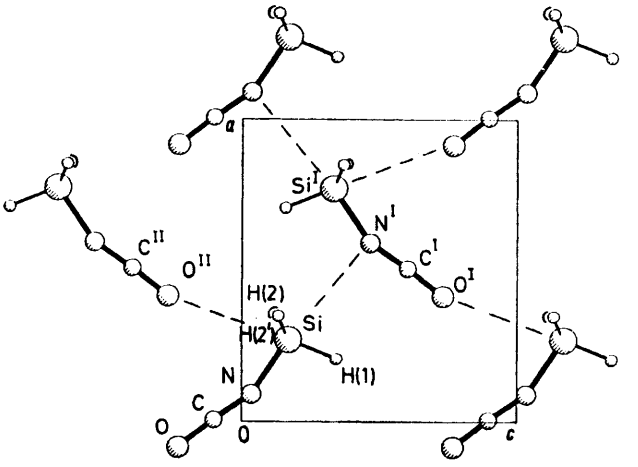

FIGURE 2 Arrangement of molecules of $SiH_3(NCO)$ on the mirror plane at $y = \frac{1}{4}$ showing the N · · · Si and O · · · Si interactions. Roman numerals as superscripts refer to the equivalent positions defined in Table 4

are probably accentuated by the use of split-film cassettes for low-temperature work. The reliability of the atomic vibration parameters is adversely affected by the lack of

* For details see Notices to Authors No. 7, *J.C.S. Dalton*, 1979, Index issue.

direct experimental data for the inter-layer scale factors. Estimated standard deviations listed in Tables 1—4 do not include contributions from errors in the cell parameters, but the results given in the abstract, in the Discussion, and in Table 5 do include such contributions.

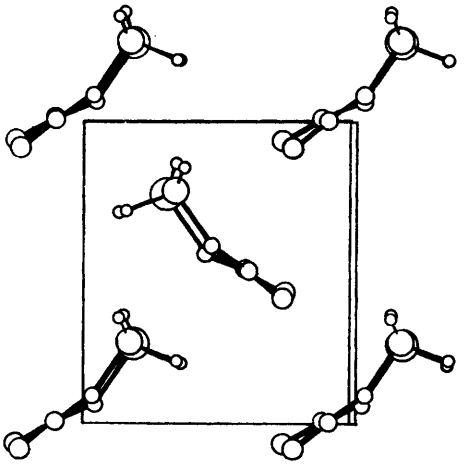

FIGURE 3 Superimposition of structure of $SiH_3(NCO)$ on that for $GeH_3(NCO)$ for molecules on the mirror planes at $y = \frac{1}{4}$

DISCUSSION

Both compounds crystallise in the same orthorhombic space group (*Pnma*) with similar unit-cell dimensions and atomic co-ordinates. In both structures the molecules have crystallographic $C_s(m)$ symmetry.

Intramolecular Geometries.—The compounds have bent, zigzag, heavy-atom skeletons where the angles at nitrogen and carbon show the greater deviations from linearity for the germyl species. Thus Ge–N–C is 147.0(7)° with N–C–O 173.8(9)°, while Si–N–C is 158.4(5)° with N–C–O 176.4(6)°. In both solid-state structures the angle at nitrogen is some 6° wider than the apparent angles measured by electron diffraction for gaseous molecules (see Table 5). The Si–N–C angle at the minimum of a proposed potential-energy function calculated from analysis of the vapour-phase i.r. spectrum is 158.8°,[8] and the *X*-ray value is very close to this. Comparison of the *X*-ray and e.d. molecular parameters indicates an apparent lengthening of the M–N bond in the crystal: Si–N increases by 0.016 Å and Ge–N increases by 0.025 Å. In $SiH_3(NCO)$ the N–C bond is longer than C–O while in $GeH_3(NCO)$ the opposite holds true. The total variation ($\Delta_1 - \Delta_2$) is 0.039 Å with an e.s.d. of 0.015 Å and is not significant, but the variation is in the direction expected for a weakening of the Ge–N relative to the Si–N bond.

TABLE 5

Molecular parameters for $MH_3(NCY)$ species

Compound	Diffraction method	Phase	Ref.	M–N/Å	M–N–C/°
$SiH_3(NCO)$	*X*-ray	Solid	This work	1.720(6)	158.4(5)
	e.d.	Gas	6	1.704(4)	152
$SiH_3(NCS)$	e.d.	Gas	6	1.705(6)	164
$SiH_3(NCSe)$	e.d.	Gas	9	1.708(6)	158.9(3)
$GeH_3(NCO)$	*X*-ray	Solid	This work	1.856(8)	147.0(7)
	e.d.	Gas	11	1.831(4)	141.3(3)

Intermolecular Geometries.—The arrangement of molecules on the mirror planes at $y = \frac{1}{4}$ and $\frac{3}{4}$ (see Figure 2) indicates two-dimensional networks of molecules orientated through long but directionally specific O · · · Si (or Ge) and N · · · Si (or Ge) intermolecular contacts. The nitrogen contact generates intermolecular angles such that N · · · M–N is close to 180° with the M · · · N vector bisecting the intramolecular M–N–C angle. For the oxygen contact the angles O · · · M–H(1) and C–O · · · M are close to 180°. Whereas the Si · · · O (3.30 Å) and Ge · · · O (3.35 Å) contacts are of similar length, the N · · · Ge contact [3.062(8) Å] is shorter than the N · · · Si contact [3.311(6) Å], and this is a particularly significant change since Ge has an atomic radius some 0.1 Å greater than Si. The increased strength of the intermolecular N · · · M interaction in the germyl structure might be associated with the more pronounced lengthening of the intramolecular Ge–N rather than the Si–N bond when comparing solid with gas-phase molecular geometries. Such behaviour would be consistent with increased acceptor character for Ge and/or increased donor character for N in $GeH_3(NCO)$ relative to $SiH_3(NCO)$.

Although the increases in the M–N bond lengths are only marginal it is important to establish a connection between the presence of intermolecular interactions in the crystalline state and possible distortion of molecular geometry. Distortions of tetrahedral MA_3X species by interaction with neighbouring atoms Y have been likened [21] to incipient S_N2 reactions involving trigonal-bipyramidal intermediates Y · · · MA_3 · · · X. In a study of X · · · CdS_3 · · · Y fragments occurring in crystal structures, Bürgi [22] found that the large variations in length of short and long axial bonds could be related to each other and also to the bond angles at Cd; the lengths of the equatorial Cd–S bonds were more or less constant and showed no systematic variation. By analogy, in crystalline $SiH_3(NCO)$ and $GeH_3(NCO)$ the intermolecular, axial, N · · · M interactions may perturb the intramolecular M–N bonds (to which N · · · M is *trans*) but the *cis*, or equatorial, O · · · M interactions would not be expected to affect the M–N bond length. [Unfortunately the H atoms in crystalline $SiH_3(NCO)$ and $GeH_3(NCO)$ are too poorly located to reveal angle distortions at Si and Ge.] Structural data from other silicon compounds (see Appendix) support the idea of a relationship between the lengths of Si · · · N interactions and distortions from tetrahedral geometry at Si. There is a clear similarity between the behaviour of Si and Cd in S_N2-type reactions in the solid state. Using methods described in the Appendix we estimate that the presence of the N · · · Si interaction in crystalline $SiH_3(NCO)$ will have increased the intramolecular Si–N bond by 0.02 Å. There is insufficient structural information about Y · · · Ge–X

fragments to derive *ab initio* correlations applicable to distortions at germanium. If, however, equation (A5) in the Appendix were applicable to N · · · Ge–N fragments (by substituting the value 1.84 Å appropriate for a Ge–N single-bond length) then the estimated perturbation to the Ge–N bond in crystalline $GeH_3(NCO)$ is +0.04 Å. Such increases could account for the marginal differences in M–N bond lengths between solid- and gas-phase molecules.

Finally, the incipient three-co-ordination at N bears comparison with the crystal structure of Ag[NCO] where the NCO group is bonded, through N, equally to two Ag atoms.[23]

APPENDIX

Relationship between Length of Si · · · N *Interactions and Distortions from Tetrahedral Geometry at* Si *in* N · · · SiA_3–X *Species.—Description of data.* Data are taken from crystal structures containing five-co-ordinated silicon atoms where at least one of the atoms bonded to silicon is nitrogen. In most of these structures four of the ligands are at more or less normal bonded distances from silicon while the nitrogen atom, the fifth ligand, is at a distance greater than the sum of covalent radii but less than the sum of van der Waals radii. Relevant distance and angle data are listed in Table 6. The data are taken from the crystal structures of 11 compounds having silatrane-type geometries [compounds (1)—(9), (11), and (12)] and of dimethylsilylamine pentamer [compound (10)]. Only those compounds whose molecular geometries are reported in journals held in our library or are available through the C.S.S.R. System [24] are included in Table 6.

In compound (10) the Si atoms are located midway along the sides of a pentagon of NMe_2 units. The Si–N distances vary from 1.94(2) to 2.09(2) Å with N–Si–N angles very close to 180°; the hydrogen atoms were not located but the average co-ordination at Si may be assumed to be trigonal bipyramidal.

The silatrane geometry facilitates the formation of short transannular N · · · Si contacts. Figure 4 illustrates the structure type. With one exception, all the silatrane compounds have N · · · Si distances in the range 2.1—2.4 Å (*i.e.* much less than the sum of van der Waals radii) and show distortions from tetrahedral bond angles at Si, and longer than normal Si–X distances. Furthermore, the shorter the

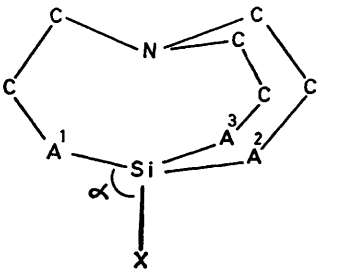

FIGURE 4 Illustration of silatrane geometry. In 1-methylsilatrane, for instance, $A^1 = A^2 = A^3$ = oxygen and X = methyl

N · · · Si distance the greater the displacement of N from the plane of its neighbouring atoms *towards* Si. In compound (11), however, the N · · · Si distance is much longer (2.89 Å), N has essentially trigonal-planar geometry, and the mean X–Si–A angle is 108.8(3)°, close to the tetrahedral value. Thus in compound (11) the N · · · Si interaction is very weak and as such represents a particularly useful datum point for this analysis. Unfortunately, this is the only compound to show a substantial deviation from the correlation presented here: the mean X–Si–A angle in compound (11) is 2.4° greater than would be predicted. This may indicate a limitation of the method used here, although it should be noted that in all the other silatrane species the axial ligand atom, X, is carbon while in compound (11) X is Pt. In any event compound (11) is not used in the following analysis.

TABLE 6

Crystal structures with N · · · SiA_3–X fragments where N · · · Si–X is approximately linear

Compound	X	Ref.	Bond distance/Å r(N · · · Si)	Bond distance/Å r(Si–X)	⟨N · · · Si–A⟩/°
(1)	Ph	26	2.132(4)	1.894(5)	83.7
(2)	Ph	*a*	2.156(4)	1.908(5)	83.2
(3)	$C_6H_4NO_2$-*m*	*b*	2.116(8)	1.904(9)	84.1
(4)	Ph	*c*	2.301(6)	1.901(6)	81.8
(5)	Me	25	2.336(4)	1.877(5)	80.2
(6)	Ph	*d*	2.344(5)	1.853(6)	79.9
(7)	CH_2Cl	*e*	2.25	1.89	84.3
(8)	Ph	*f*	2.193(5)	1.882(6)	82.9
(9)	CH_2Cl	*g*	2.111	1.921	84.7
(10)	NMe_2	*h*	1.984 [i]	1.984	90 [j]
(11)	$PtCl(PMe_2Ph)_2$	*k*	2.89(1)	2.292	71.2
(12)	Me	*l*	2.175(4)	1.870(6)	82.7

[a] L. Párkányi, K. Simon, and J. Nagy, *Acta Cryst.*, 1974, **B30**, 2328. [b] J. W. Turley and F. P. Boer, *J. Amer. Chem. Soc.*, 1969, **91**, 4129. [c] J. J. Daley and F. Sanz, *J.C.S. Dalton*, 1974, 2051. [d] F. P. Boer, J. W. Turley, and J. J. Flynn, *J. Amer. Chem. Soc.*, 1968, **90**, 5102. [e] A. Kemme, J. Bleidelis, I. Solomennikova, G. Zelchan, and E. Lukevics, *J.C.S. Chem. Comm.*, 1976, 1041. [f] J. W. Turley and F. P. Boer, *J. Amer. Chem. Soc.*, 1968, **90**, 4026. [g] A. A. Kemme, J. J. Bleidelis, V. M. Djakov, and M. G. Voronkov, *Zhur. strukt. Khim.*, 1975, **16**, 914. [h] R. Rudman, W. C. Hamilton, S. Novick, and T. D. Goldfarb, *J. Amer. Chem. Soc.*, 1967, **89**, 5157. [i] Average value for the pentamer; all the Si–N distances are approximately equal. [j] Assumed value; the 'equatorial' ligands are hydrogen and were not located. [k] C. Eaborn, K. J. Odell, A. Pidcock, and G. R. Scollary, *J.C.S. Chem. Comm.*, 1976, 317. [l] L. Párkányi, L. Bihátsi, and P. Hencsei, *Cryst. Struct. Comm.*, 1978, **7**, 435.

Structural correlations. The inter-relationship of distortions in silatrane compounds has already been noted, in a qualitative way, by Boer and Turley [25] and by Párkányi *et al.*[26] We now establish a simple quantitative relationship for application to our studies of intermolecular N · · · Si interactions occurring in the crystal structures of silicon

compounds. The treatment is analogous to, and incorporates the assumptions of, the method used by Bürgi [22] for relating bond-length and -angle distortions in Y · · · CdS_3 · · · X fragments.

Figure 5 is a scatter plot of the Si · · · N and Si–X distances against the angles α, where α is the mean N · · · Si–A angle (see Figure 4). It shows that as *r*(Si · · · N) decreases so *r*(Si–X) increases slightly and α increases. [Note that the Si–X distances are not corrected for differences in atomic radii of different X atoms. Except for compound (10), the Si–X distances show little variation, nor is much variation to be expected due to the nature of equation (A4), see later.] The data may be regarded as structural illustrations of a reaction pathway leading from a tetrahedral four-co-ordinated Si atom to a trigonal-bipyramidal five-co-ordinated species.

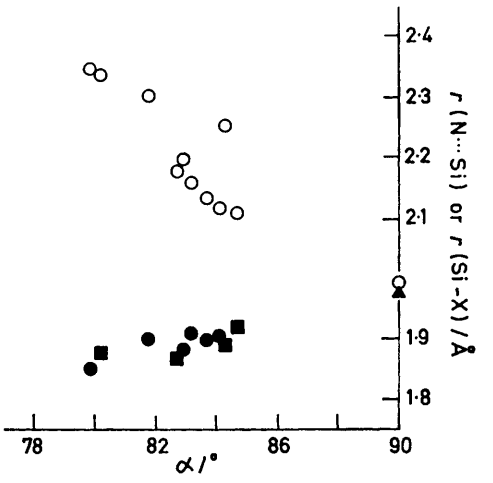

FIGURE 5 Scatter plot of *r*(N · · · Si), open circles, and *r*(Si–X) [X = C(sp^2) (●), C(sp^3) (■), or N (▲)] against α

The N · · · Si distances are assigned bond numbers, *n*(N · · · Si), assuming a linear relationship between bond number and distortion from tetrahedral bond angles at Si: $n(\mathrm{N}\cdots\mathrm{Si}) = (\Delta^t - \Delta)/2\Delta^t$, where Δ is the displacement of Si from the equatorial plane defined by the three A ligands (positive Δ is a displacement towards X), and Δ^t is the displacement appropriate for a SiA_3X group having regular tetrahedral angles. We note that equation (A1) is applicable.

$$n(\mathrm{N}\cdots\mathrm{Si}) = \frac{\Delta^t - \Delta}{2\Delta^t} = \tfrac{1}{2} - \frac{\Delta}{2\Delta^t} = \tfrac{1}{2} - \frac{\cos\alpha}{2\cos\alpha^t} \approx \tfrac{1}{2} - \frac{3}{2}\cos\alpha \quad \text{(A1)}$$

The Si–X distances may also be related to the angles α, and to the N · · · Si distances, if we assume that the sum of bond numbers for the axial bonds is constant [equation

$$n(\mathrm{N}\cdots\mathrm{Si}) + n(\mathrm{Si}\text{–}\mathrm{X}) = K \quad \text{(A2)}$$

(A2)]. It is reasonable to set *K* equal to unity although the justification is empirical: it seems to work here and for

$$n(\mathrm{Si}\text{–}\mathrm{X}) = 1 - n(\mathrm{N}\cdots\mathrm{Si}) = 0.5 + 1.5\cos\alpha \quad \text{(A3)}$$

X · · · CdS_3 · · · Y.[22] Therefore we can write expression (A3). If the N · · · Si and Si–X distances are placed on a common scale, by subtracting the single-bond covalent radii for silicon (1.17 Å),[27] nitrogen (0.70 Å),[27] carbon, sp^3-hybridised (0.77 Å),[27] and carbon, sp^2-hybridised (assumed 0.75 Å), as appropriate, then all the structural information may be fitted to a single plot, equation (A4), where Δ*r* are

$$\Delta r = c \log n + d \quad \text{(A4)}$$

distance increments for the N · · · Si and Si–X bonds and *n* is expressed in terms of the angle α by equations (A1) or (A3) as appropriate. Equation (A4) is analogous to the bond length–bond number relationship proposed by Pauling.[28] Figure 6 shows a plot of equation (A4) where the least-squares best line has $c = -1.11$ and $d = -0.22$ Å. The value of *c* determined here does not differ significantly from the value (−1.05) derived for Y · · · CdS_3 · · · X fragments.[22]

It is surprising that the general trend for Si is so well defined and its similarity with the Cd system so marked. First, bonds to Si are presumably more covalent in character than bonds to Cd: so individual Si species might be expected to be more susceptible to substituent effects, thus confusing the overall picture. Secondly, additional distortions might arise from geometric constraints imposed by the cyclic silatrane systems.

Comparison of molecular geometries in the gas and in the crystal. Most molecular species solidify to form crystal lattices where the intermolecular distances are close to or greater than the sum of van der Waals radii. Here the crystal-packing forces may affect the intramolecular geometry relative to gas-phase molecules but any changes are usually rather small and often difficult to rationalise. However, in some compounds, such as $SiH_3(NCO)$ and $GeH_3(NCO)$, the intermolecular distances in the crystal may be divided into two categories: (*a*) those at or greater than the sum of van der Waals radii; and (*b*) those appreciably

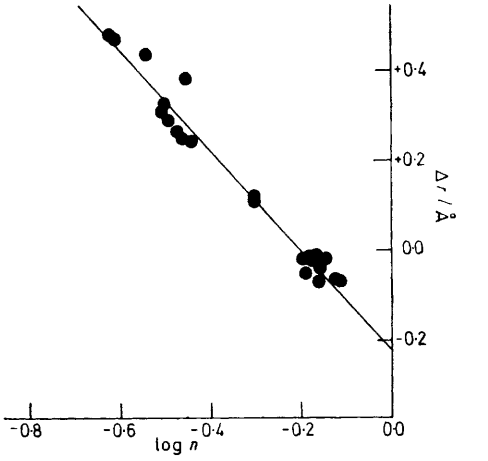

FIGURE 6 Plot of Δ*r* against log *n*, where Δ*r* are distance increments for N · · · Si and for Si–X separations, and log n = log (0.5 − 1.5 cos α) or log (0.5 + 1.5 cos α) respectively

less than the sum of van der Waals radii. In many cases these shorter contacts seem to be stereochemically specific and imply an expansion of the co-ordination sphere of some atom through the formation of ' secondary ' bonds. Here there is the possibility of more substantial change to the intramolecular geometry, and the nature of the change can be understood in terms of simple ideas about structural behaviour. Study of these intermolecular interactions

provides important insight into structural character. Thus the presence of weak secondary bonds in some silicon and germanium compounds may be seen as an expression of the tendency towards higher co-ordination number in compounds of the heavier Group 4 elements.

The previous section considered Si atoms in incipient five-co-ordination and established an empirical relationship between the length of N · · · Si contact, the length of the *trans*-Si–X bond, and the bond angles at Si. This relationship might be used to estimate how an intermolecular N · · · Si interaction will affect the intramolecular geometry in the crystal relative to the geometry in the gas phase (where there is no association between molecules), but there are some problems. First, the relationship represents a general trend and there may be appreciable deviations from this in individual cases. Secondly, there is appreciable variation in the co-ordination geometry at silicon in different compounds even when measured in the gas phase. So purely intramolecular effects are important too. Thirdly, in crystalline $SiH_3(NCO)$ and in other silyl species where hydrogen atoms are not well located the bond angles at silicon cannot be used for calculating the strength of interaction by equating the angle α with bond number. The best that may be achieved is an estimation of the probable perturbation to the intramolecular geometry, and then to see if this is in accord with any differences between the gas-phase and solid-state molecular structures.

The calculation procedure adopted for $SiH_3(NCO)$ is as follows. The bond number of the intermolecular N · · · Si interaction in the crystal is calculated using the bond length–bond number equation (A5) due to Pauling.[28] Here

$$r = r_0 + c \log n \qquad \text{(A5)}$$

r is 3.311 Å, r_0 (the length of a Si–N single bond) is taken as 1.74 Å, and c is −1.11 as determined earlier, which gives $n = 0.04$. We therefore assume that the N · · · Si interaction will have reduced the bond number for the intramolecular Si–N bond by 0.04 relative to gas-phase molecules. The resulting perturbation to the Si–N bond length in the crystal is calculated from equation (A6) where δn is

$$\delta r = (\delta n/n)c \log_{10} e \qquad \text{(A6)}$$

−0.04, n is assumed to be 1.0, c is = −1.11, and δr is calculated as +0.02 Å (for the transition, gas to crystal).

We thank the S.R.C. for support, and Dr. S. Cradock and Mr. S. G. D. Henderson for samples of the compounds and helpful discussions.

[9/1827 *Received*, 15*th November*, 1979]

REFERENCES

[1] A. Stock and K. Somieski, *Berichte d. D. Chem. Gesellshaft*, 1921, **54**, 740.
[2] K. Hedberg, *J. Amer. Chem. Soc.*, 1955, **77**, 6491.
[3] D. W. W. Anderson, D. W. H. Rankin, and A. Robertson, *J. Mol. Structure*, 1972, **14**, 385.
[4] A. G. MacDiarmid and A. G. Maddock, *J. Inorg. Nuclear Chem.*, 1955, **1**, 411; A. G. MacDiarmid, *ibid.*, 1956, **2**, 88.
[5] K.-F. Dössel and D. H. Sutter, *Z. Naturforsch.*, 1977, **A32**, 473.
[6] C. Glidewell, A. G. Robiette, and G. M. Sheldrick, *Chem. Phys. Letters*, 1972, **16**, 526.
[7] J. A. Duckett, A. G. Robiette, and I. M. Mills, *J. Mol. Spectroscopy.*, 1976, **62**, 34.
[8] S. Cradock and D. C. J. Skea, *J.C.S. Faraday II*, 1980, 860.
[9] A. A. Fraser and D. W. H. Rankin, personal communication.
[10] J. R. Durig, Y. S. Li, and J. F. Sullivan, *J. Chem. Phys.*, 1979, **71**, 1041.
[11] J. D. Murdoch, D. W. H. Rankin, and B. Beagley, *J. Mol. Structure*, 1976, **31**, 291.
[12] J. R. Durig and J. F. Sullivan, *J. Mol. Structure*, 1979, **56**, 41.
[13] M. J. Barrow, E. A. V. Ebsworth, and M. M. Harding, *Acta Cryst.*, 1979, **B35**, 2093.
[14] M. J. Barrow, S. Cradock, E. A. V. Ebsworth, and M. M. Harding, *J.C.S. Chem. Comm.*, 1977, 744.
[15] SHELX-76, Program for Crystal Structure Determination, G. M. Sheldrick, University Chemical Laboratory, Cambridge.
[16] R. F. Stewart, E. R. Davidson, and W. T. Simpson, *J. Chem. Phys.*, 1965, **42**, 3175.
[17] 'International Tables for *X*-Ray Crystallography,' Kynoch Press, Birmingham, 1974, vol. 4, (*a*) p. 99; (*b*) p. 149.
[18] D. T. Cromer and J. B. Mann, *Acta Cryst.*, 1968, **A24**, 321.
[19] *X*-Ray '72,' Technical Report TR-192, University of Maryland, 1972.
[20] PLUTO, Program for Plotting Crystal and Molecular Structures, W. D. S. Motherwell, University Chemical Laboratory, Cambridge.
[21] H.-B. Bürgi, *Angew. Chem. Internat. Edn.*, 1975, **14**, 460.
[22] H.-B. Bürgi, *Inorg. Chem.*, 1973, **12**, 2321.
[23] D. Britton and J. D. Dunitz, *Acta Cryst.*, 1965, **18**, 424.
[24] Crystal Structure Search Retrieval, P. A. Machin, J. N. Mills, O. S. Mills, and M. Elder, Daresbury Laboratory, Science Research Council, Daresbury, Warrington.
[25] F. P. Boer and J. W. Turley, *J. Amer. Chem. Soc.*, 1969, **91**, 4134.
[26] L. Párkányi, J. Nagy, and K. Simon, *J. Organometallic Chem.*, 1975, **101**, 11.
[27] L. Pauling, 'The Nature of the Chemical Bond,' 3rd edn., Cornell University Press, Ithaca, New York, 1960, p. 246.
[28] L. Pauling, *J. Amer. Chem. Soc.*, 1947, **69**, 542.